Chapter 5

Diffractive objective lens

5.1 Introduction

The reflow process can not make an arbitrary lens profile with uniform refractive indexes. Therefore, the other process, gray-scale mask photolithography is proposed. With well-adjusted aperture ratio on the mask, the profiles of aspheric surface are achievable.

The first kind of lens with aspheric profile is aspheric lens. However, the thickness of the aspheric lens is too large for fabrication by using AZ4620 as lens material. Therefore, a Fresnel lens with much smaller thickness can be used to replace the refractive aspheric lens. However, generally for a Fresnel lens is concerned, the linewidth of the outmost fringe of 1 μm is too small to be fabricated. Therefore, a harmonic lens is proposed.

The harmonic element is exploited for making a thin focal lens. Such elements are composed of rings of an equal depth but different diameter and surface profile to focus light. The corresponding diffractive fringes of a classical refractive lens are depicted in Fig. 5-1 [1]. There are three basic steps to determine the fringes pattern of the diffractive surface.

(a) Obtain the analytical expression of the refractive phase profiles;

(b) Slice the phase profile into $2m\pi$ wide layers (modulo $2m\pi$ lens);

(c) Finally, compress the modulo $2m\pi$ phase.

When we use this approach to design a lens, spherical aberration is introduced and will be discussed in this chapter. A new approach to design harmonic lenses is

proposed to overcome the aberration induced by slicing.

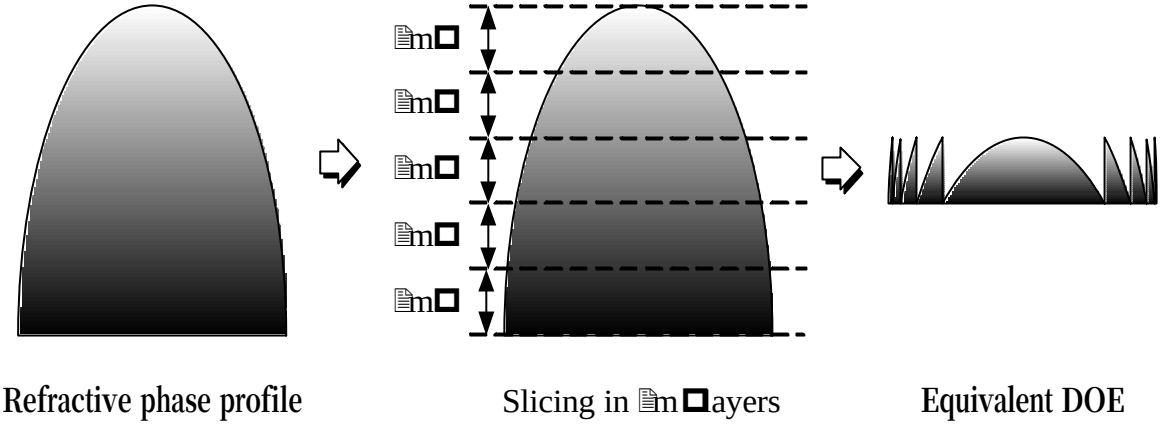

(a) (b) (c)

Fig. 5- 1 Phase profile slicing steps (a) refractive phase profile (b) slicing into layer with $2m\pi$ phase shift and (c) equivalent DOE

5.2 Aspheric Lens

To eliminate the spherical aberration of a focusing lens, an aspheric surface which can be fabricated with gray-scale mask as discussed in Chapter 3 will be exploited. Considering the DVD specification with a cover layer of 0.1 mm, the focal length must be theoretically larger than 62.5 μm which is the equivalent air thickness of the cover layer with refractive index of 1.6. Moreover, for the thickness of lens and working distance, the focal length larger than 62.5 μm is needed. However, in order to make a compact system, the system must be as small as possible. When the focal length becomes shorter, the effects of disk tilt and larger field angle become stronger. Considering the cover layer thickness of 0.1 mm and NA of 0.6, a convex-plane aspheric lens is designed by using optimization approaches described in Chapter 2. For D = 250 μm, n = 1.8, and NA = 0.6, the focal length is 166.15 μm. The working distance and lens thickness are 50 μm and 97.5 μm, respectively. The lens parameters

are shown in Tab. 5- 1.

Tab. 5- 1 Convex-plane aspheric lens parameters of front and back surface

Lens Parameter	Front Surface
cv (mm^{-1})	7.52
cc	-1.04
ad (mm^{-1})	26.86
ae (mm^{-3})	701.22
af (mm^{-5})	$-19.71\ 10^{3}$
th (μm)	97.5

cv and cc denotes the curvature and the conic constant of the front surface of the convex-plane aspheric lens; as, ae, and af denote the coefficients for higher order terms; th is the thickness of the aspheric lens. The optical performance evaluated with the spot diagram, optical path difference, and point spread function are depicted in Fig. 5- 2(a), (b), and (c) respectively. The spot diagram shows that the lens is nearly aberration free because spot radius is smaller than the Airy disk radius of 0.625 μm. Next, the point spread function computes the intensity of the diffraction image formed by the optical system for a single point source in the field. The FWHM of the exact spot size considering the diffraction effect is about 1 μm. The maximum optical path difference of 0.04 ? meets the DVD specification for objective lens.

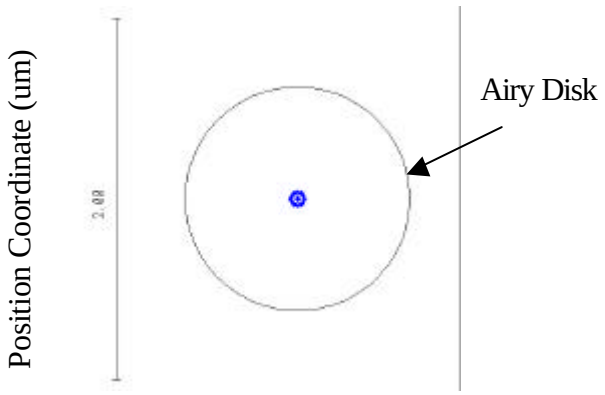

(a)

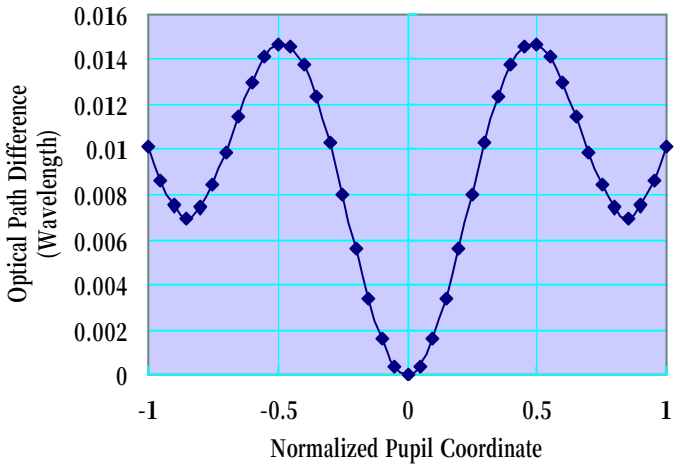

(b)

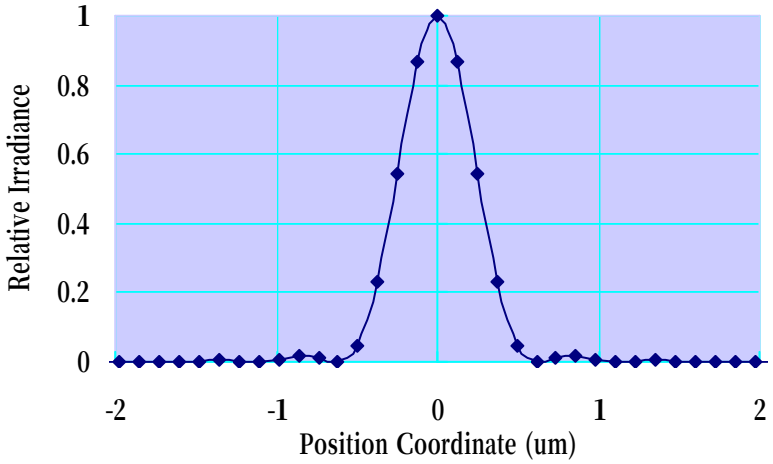

(c)

Fig. 5- 2 Aspheric lens performance of (a) spot diagram, (b) optical path difference, and (c) point spread function

5.3 Fresnel Lens

A Fresnel lens is a thin optical element which can be used for objective lens of DVD and is composed of diffractive zones with each zone of a 2π phase shift and continuous relief in each zone segment. The optical path difference between adjacent rings is ?. The lens profiles within each zone are tailored to make all the rays pointing toward the same focal point.

5.3.1 Diffractive

The Fresnel lens is illustrated in Fig. 5- 3. The jth Fresnel zone radius can be calculated by the phase difference between the jth zone and the axial ray in the form of Eq. 5-6.

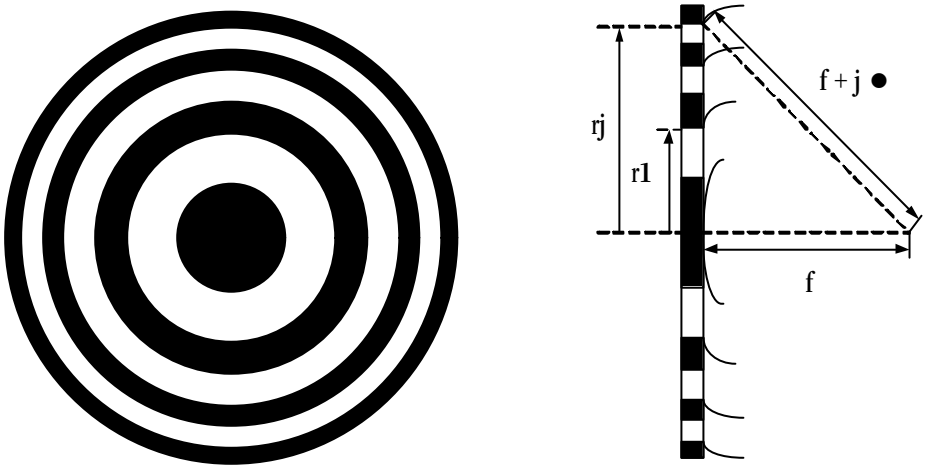

(a) (b)

Fig. 5- 3 Arrangement of the annular rings in Fresnel lens: (a) texture of the Fresnel zone plate and (b) optical path differences between light rays from different zones

the phase difference between the jth zone and the axial ray [2]

$$\Phi_{ideal}(r_j) = \frac{2p}{l}(f - \sqrt{f^2 + r_j^2}) = j2p \qquad \text{(Eq. 5-6)}$$

Therefore,

$$r_j = \sqrt{2jlf + (jl)^2} \qquad \text{(Eq. 5-7)}$$

For $(jl)^2 << 2jlf$

$$r_j = \sqrt{2jlf} \qquad \text{(Eq. 5-8)}$$

With paraxial approximation, the fabrication consideration is discussed below. The number of zones M can be determined by Eq. 5-9. [2]

$$\frac{2p}{l}(\sqrt{R^2 + f^2} - f) = 2Mp$$

$$M = \frac{R}{l}(\sqrt{1+(F/\#)^2} - 2(F/\#)) = \frac{R}{4l(F/\#)} \qquad \text{(Eq. 5-9)}$$

Where F/# and 2R are the f-number of lens and the Fresnel lens diameter respectively. The relation between numerical aperture and F/# is

$$NA = \frac{1}{\sqrt{1+4(F/\#)^2}} \cong \frac{1}{2(F/\#)}$$

$$M = \frac{R}{2l}NA \qquad \text{(Eq. 5-10)}$$

Furthermore, the minimum feature size of Fresnel lens is derived. For a given wavelength (?), the minimum feature $w_{\min}$ is

$$w_{\min} = R_M - R_{M-1} = \sqrt{2Mfl + M^2l^2} - \sqrt{2(M-1)fl + (M-1)^2l^2}$$

$$= \frac{l}{R}(f + Ml)$$

For $M = \frac{R}{2l}NA$,

$$w_{\min} \cong \frac{l}{NA} \qquad \text{(Eq. 5-11)}$$

For NA=0.6, ? = 650 nm, lens diameter 2R=260 μm,

$$M = \frac{130}{2\times 0.65}0.6 = 60$$

$$w_{\min} = 1.08mm$$

5.3.2 Surface relief of Fresnel lens

With the continuous phase, all the rays will reach the same phase at the focal point indicated in Fig. 5- 4.

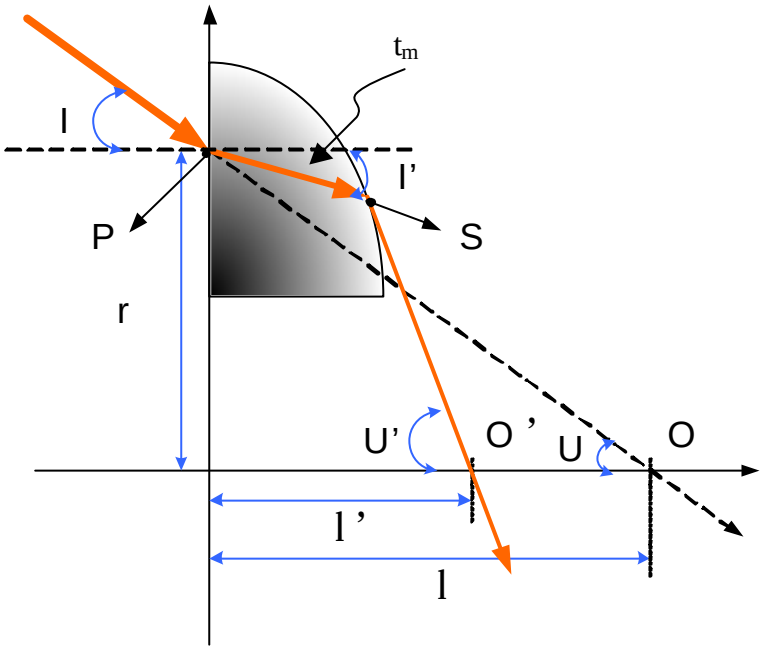

Fig. 5- 4 Schematic diagram of Fresnel lens shape

The Fresnel lens is used to collect the light emerge from the object onto the image. The refractive shape of Fresnel lens can be derived from the optical path difference between the axial ray and an arbitrary ray shown as a solid line in Fig. 5- 4. In Fig. 5- 4, the point O and point O' denote the object and image position. The optical path of ray hit the lens at point P is denoted as [O R S O']. The optical path difference (OPD) of the two rays, the ray on the axis and the ray indicated in solid line must be of modulo PSl .

$$[\text{O R S O'}] = l - l' + PSl$$

$$\begin{cases} P = m \\ P = m-1 \end{cases} \text{ and } \begin{cases} S = 1 \\ S = -1 \end{cases} \text{ for } \begin{matrix} f' > 0 \\ f' < 0 \end{matrix} \qquad \text{(Eq. 5-12)}$$

Where f' is the focal length of Fresnel lens. For a positive lens, focal length f'

must be larger than 0.

$$\frac{r}{SinU} + nt_m + \sqrt{(l' - t_m CosI')^2 + (r + t_m SinI')^2} = l' - l + PSl \qquad \text{(Eq. 5-13)}$$

t_m is the length of light propagating inside the lens. According to Snell's law,

$$SinI' = \frac{1}{n} SinI = \frac{-1}{n} SinU \qquad \text{(Eq. 5-14)}$$

$$CosI' = \frac{1}{n}\sqrt{n^2 - (SinU)^2} \qquad \text{(Eq. 5-15)}$$

Thus, Eq. 5-12 becomes

$$(l' - t_m CosI')^2 + (r + t_m SinI')^2 = (T + PSl + \frac{r}{SinU} - nt_m)^2 \qquad \text{(Eq. 5-16)}$$

Where T = l'-l. Eq. 5-16 can be rearranged as

$$(n^2 - 1)tm^2 + 2[l'CosI' - rSinI' - n(T + PSl + \frac{r}{SinU})]t_m + (T + PSl + \frac{r}{SinU})^2 - l'^2 - r^2 = 0$$

(Eq. 5-17)

$$At_m^{\ 2} + Bt_m + C = 0 \qquad \text{(Eq. 5-18)}$$

$$A = n^2 - 1$$

$$B = -2n(T + PSl + \sqrt{r^2 + l^2}) + 2 \times \frac{1}{n}[(T + l)\sqrt{n^2 - \frac{r^2}{l^2 + r^2}} + \frac{r}{\sqrt{l^2 + r^2}}]$$

$$C = -2T(l - PSl - \sqrt{l^2 + r^2}) + (Pl)^2 + 2PSl\sqrt{l^2 + r^2}$$

t_m then can be solved from Eq. 5-18. Consequently, for a given refractive index n, wavelength ?, T=l'-l and l, t_m is a function of r. In addition, the thickness of the Fresnel lens is $\frac{l}{n-1}$. The thickness is available for coating the photoresist AZ4620.

When using a pure diffractive device such as Fresnel lens to focus light, some issues should be considered. First, For NA=0.6, ? = 650 nm, lens diameter 2R=260 μm, the feature size of 1 μm is too small for geometric ray tracing to be valid and fabrication to be achievable. In addition, the depth of focus is very short. It's not feasible to use Fresnel lens as objective lens of high NA.

5.4 Harmonic diffractive lens

5.4.1 Direct sliced objective lens

Due to the limitation of 50 μm maximum spin coating thickness of AZ4620 [3], the aspheric lens with thickness of 97.5 μm designed in Section 5.2 is not feasible. Moreover, when using a pure diffractive device such as Fresnel lens to focus light, the outmost fringe width is too small to be fabricated for an objective lens of high NA.

To reduce the thickness of lens and enlarge the feature size, the shape of the lens has been sliced into pieces of $2m\pi$ phase modulo where m is an integer larger than 1. This kind of lens is called harmonic diffractive lens [4]. The harmonic lenses differ from the Fresnel lenses in the way of encoding. The height of the harmonic lens corresponds to a phase of modulo $m2\pi$ (where m is an integer, $m \geqq 1$) rather than 2π for a reference wavelength ?. As a consequence, the harmonic lenses allow larger linewidth and give deeper grooves than regular diffractive optical elements (DOEs) without increasing the aspect ratio of the groove profile, since the linewidth and the depth are enlarged by a similar factor.

The behavior of harmonic lens is the resultant effect of refractive and diffractive nature of the surface. The diffraction redistributes the energy and reduces the central intensity. To examine the feasibility of the harmonic lens, a surface of 2π phases sliced is simulated by using ASAP.

To perform the simulation of harmonic lens, the aspheric coefficients computed by ZEMAX are put into the aspheric surface polynomials (Eq. 2-12). Then, the rings for Fresnel lens are calculated by solving the equation of aspheric surface below.

$$(n-1)\frac{cvr_m^{\ 2}}{1+\sqrt{1-cv(cc+1)r_m^{\ 2}}}+ad\times r^4+ae\times r^6+af\times r^8=ml \qquad \text{(Eq. 5-19)}$$

The first ten rings are shown in Tab. 5-2.

Tab. 5- 2 The first ten ring radii of slicing harmonic lens

m	r (m) (μm)
1	20.26
2	28.65
3	35.08
4	40.50
5	45.27
6	49.58
7	53.53
8	57.22
9	60.68
10	63.94
Minimum linewidth	0.72

Then, the lens profile is drawn and ray-traced is performed, and the result is shown in Fig. 5- 5 (a) where the geometrical aberration is obvious due to the slicing steps. The dashed circle in the figure highlights the focal shift. As shown in Fig. 5- 5 (b), the geometrical aberration is illustrated with spot size being larger then Airy disk radius of 1 μm due to the shift of the point where the rays bend toward the focal point. In fact, the spot size is about 290 μm which is much larger than the spot size for DVD application of 1.08 μm. Moreover, 0.33% energy of incident light can be collected within the dashed circle shown in Fig. 5-5 (b). Therefore, the spherical aberration of directly sliced harmonic lens is obvious.

The spherical aberrations which occur due to the ray shift of the inner profile of the aspheric surface can be explained in detail. In Fig. 5- 6, the dash and solid rays denote the light passing through the lens before and after slicing. The aberrations occur due to the ray shift of inner part of aspheric lens from ideal focal point A to

point B. Moreover, the surface relief is simplified with blazed profiles. The deviations between the exact shape and approximate blazed lens shape introduce aberration, too.

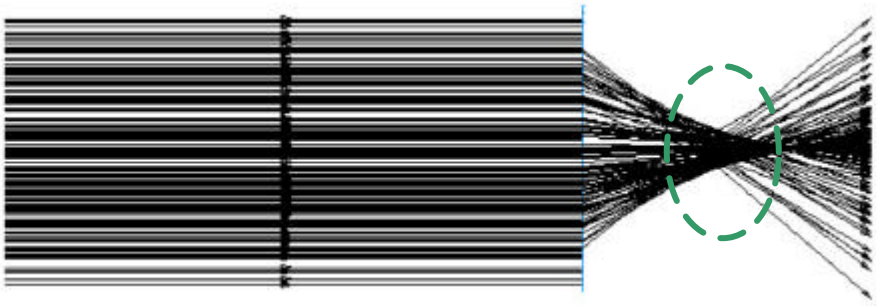

(a)

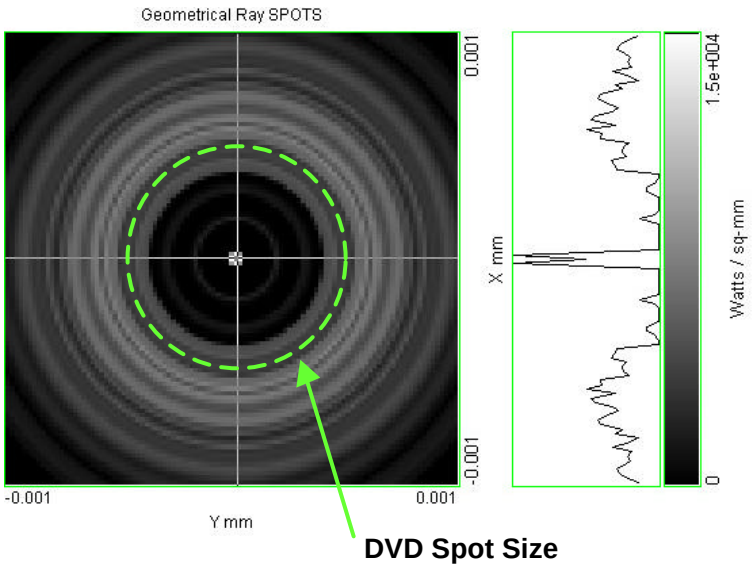

(b)

Fig. 5- 5 (a) Simulation results of aberration and (b) illumination plot for sliced harmonic lens

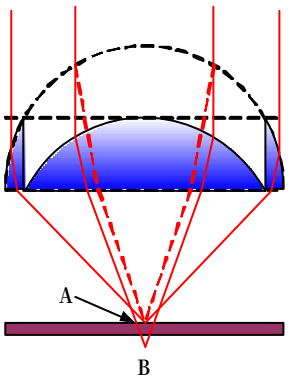

Fig. 5- 6 Schematic diagram of aberration of focal shift

5.4.2 Hybrid aspheric harmonic objective lens

To overcome the problems mentioned above, a new method is proposed to generate the annular zones which are the combination of segments of optimized aspheric profile. The approach of estimating the paraxial parameters is illustrated in Fig. 5- 7. For the original refractive lens of the harmonic lens, the thickness th can be calculated with paraxial approximation for a given focal length f, lens diameter D, and refractive index of material n.

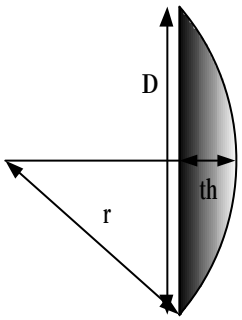

Fig. 5- 7 Lens parameters for paraxial calculation

The geometry gives the relationship

$$(\frac{D}{2})^2 + (r-h)^2 = r^2 \qquad \text{(Eq. 5-20)}$$

$$r = \frac{(\frac{D}{2})^2 + h^2}{2h} \qquad \text{(Eq. 5-21)}$$

for F-number = F/#,

$$f/D = \text{F/\#}$$

where f is the focal length of the lens, and

$$f = r/n-1$$

Therefore, the thickness of lens can be calculated.

$$h^2 - 2h(n-1)(F/\#)D + (\frac{D}{2})^2 = 0 \qquad \text{(Eq. 5-22)}$$

therefore, h is in the form of Eq. 5-23.

$$h = D\left(\frac{2(n-1)(F/\#) \pm \sqrt{(2(n-1)(F/\#))^2 - 1}}{2}\right) \qquad \text{(Eq. 5-23)}$$

For NA = 0.6 (F/# = .667), n = 1.8,

$$h = 0.348D$$

To make a harmonic lens, the precise value of thickness should be adjusted to integer multiple of 10 ? (wavelength) to avoid diffraction. Besides, for three beams tracking, the distance of 25 µm between the zero order and the first order beam spot should be taken into consideration in determining the lens diameter of 50 µm larger than the beam width. Taking D = 260 µm as an example, the thickness h calculated from Eq. 5-23 is 87 µm. From simulation result, to reach aberration-free lens with aspheric surface, the applicable thickness is in the vicinity of 78 µm which is a multiple of 10 ?. The approach of designing harmonic lenses is illustrated in Fig. 5- 8. By fixing the working distance in slicing the lens profile, the zone diameter and aspheric lens thickness are changed to obtain each zone profile. The aspheric lens is designed with diameter r_1 of 260 µm, thickness of 78 µm, working distance of 50 µm, made with AZ4620 of n=1.8. The lens parameters of aspheric profile are optimized following the optimization flow chart described in Chapter 2. The aspheric coefficient is well-adjusted to eliminate the aberrations. Then, the lens profile is sliced into several pieces of 19.5 µm (30?) height and the outermost segment circle is kept as the first zone (Fig. 5- 8(a)). The aspheric coefficient of the first zone is put into the Eq. 5-20 to calculate the second zone diameter r_2. After that, the second aspheric profile with diameter $2r_2$ and thickness of 58.5 µm is redesigned. Again, the surface is sliced into several pieces with height of 19.5 µm and the third zone diameter is computed. The iteration is done until the last zone is achieved as shown in Fig. 5- 8(c).

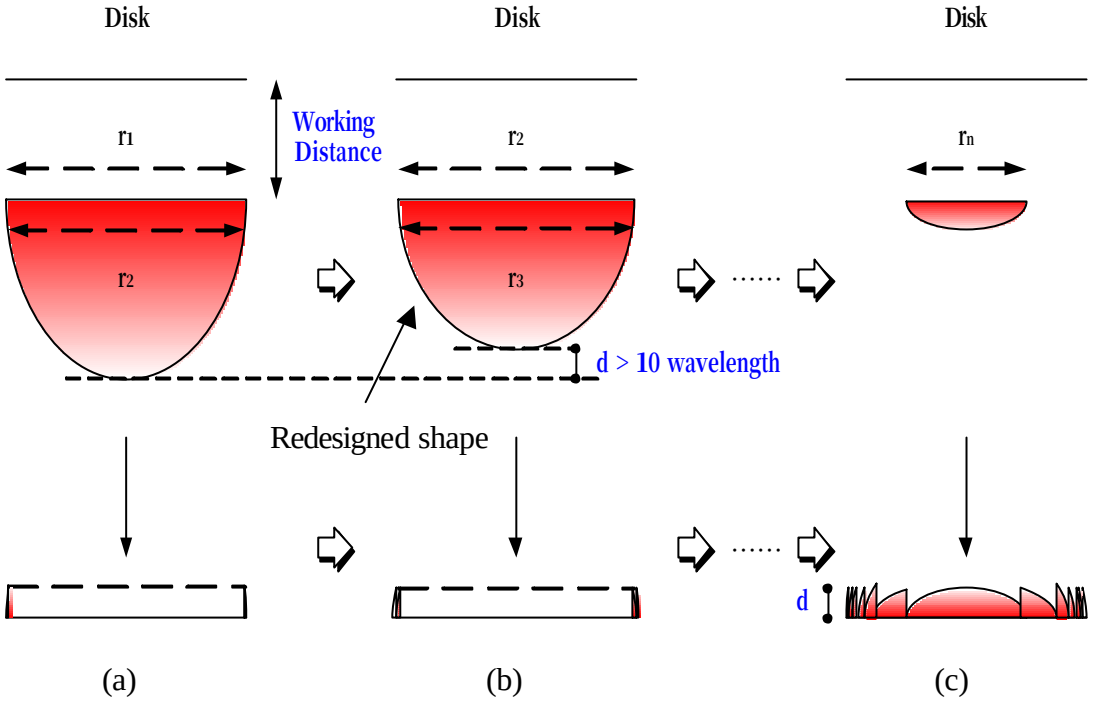

Fig. 5- 8 The approaches of slicing (a), (b), and (c)

To design a system for three beam tracking, the extra field angle should be given. The angle is defined by tan [A/B], where A and B are [the distance between the objective lens and the grating which is used for splitting laser beam] and [the separation of the first order and the zero order diffraction spots] respectively. In our design, the field angle is tan [(2mm) / (25μm)] = 0.7 degree. In addition, for a lens diameter of 260 μm, the maximum beam width without vignetting is 210 μm. The aspheric coefficients and performances of zones are tabulated in Tab. 5- 3 and Tab. 5-4, respectively. The optical performance of the first zone is shown in Fig. 5- 9.

Tab. 5- 3 Aspheric parameters for each zone

radius	diameter/2 (mm)	cv (mm^{-1})	cc	ad (mm^{-1})	ae (mm^{-3})	af (mm^{-5})
r_1	1.30E-01	1.24E-01	-9.57E-01	2.20E+01	1.65E+03	-6.38E+04
r_2	1.14E-01	1.10E-01	-9.61E-01	-1.05E+02	2.54E+04	-1.39E+06
r_3	9.10E-02	1.02E-01	-1.02E+00	-1.44E+02	5.67E+04	-5.13E+06
r_4	6.30E-02	9.90E-02	-3.50E-01	-3.44E+01	2.18E+04	-1.44E+07

Tab. 5- 4 Optical performances for each zone of the redesigned harmonic lens

spot diagrams	Airy disk (μm)	RMS radius (on axis) (μm)	Strehl ratio	Maxima OPD (λ)
r1	1.17	0.22	0.90	0.20
r2	1.29	0.71	0.55	0.40
r3	1.59	0.28	0.95	0.12
r4	5.12	0.001	1.00	<0.002

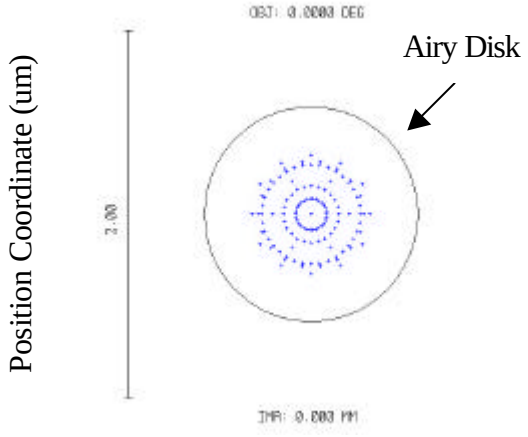

(a) Spot diagram of the first zone

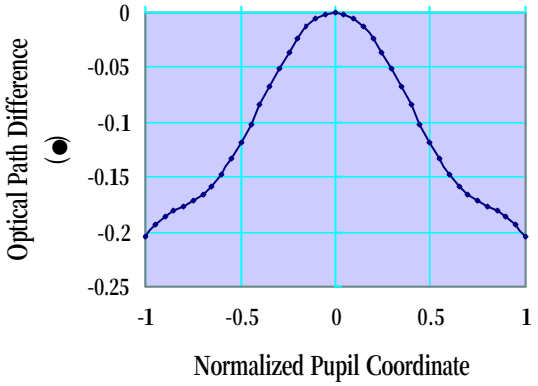

(b) Optical path difference of the first zone

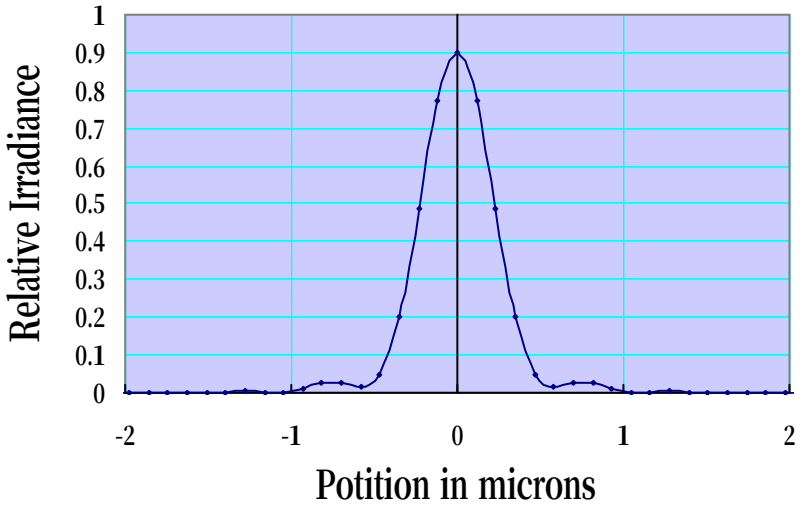

(c) Point spread function of the first zone

Fig. 5- 9 Layout and performances of (a) spot diagram, (b) optical path difference, and (c) point spread function of the first segment

In Fig. 5-9 (a), the size of focused spot of the first segment is smaller than the Airy disk. Therefore, the geometrical aberration of the first segment is negligible. Moreover, in Fig. 5-9 (b), optical path difference of the focused spot at the focal plane is 0.2 ? which meets the Rayleigh criteria of 0.25 ?. From the point spread function as shown in Fig. 5-9 (c), the spot size of the first segment is about 1 μm.

To examine the overall performance of the harmonic lens which is the combination of four segments, the harmonic lens of comprising the zones with aspheric shape is analyzed with ASAP as shown in Fig. 5- 10. From the density distribution based on geometrical ray-tracing as shown in Fig. 5- 11, the spot size smaller than Airy disk indicates that the geometrical aberration has been corrected by redesigned aspheric surfaces. Comparing Fig. 5- 10 with Fig. 5- 5 (b), the spot size of 0.01 μm is minimized. In other words, the aberrations resulted from slicing have been corrected. Because most zones are surface with eliminated geometrical aberrations, the lens performance is very close to diffraction limit. The equivalent NA of 0.634 is determined by the ratio of D/2f, where D is the outermost segment diameter and f is the effective focal length. Moreover, according to the diffraction theory, the minimum spot size proportional to ?/NA is 1.062 μm.

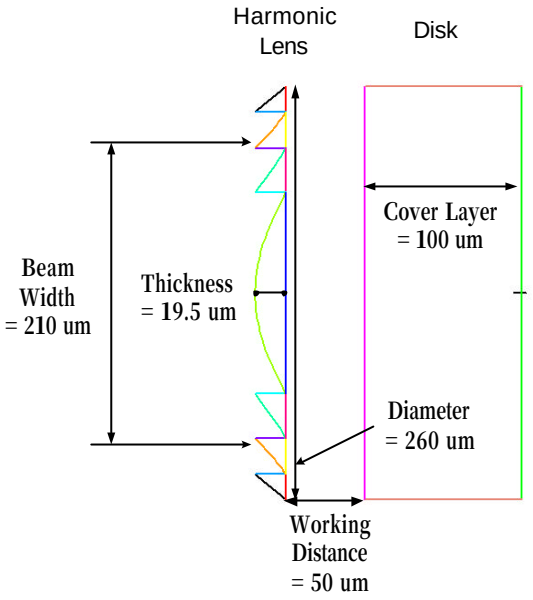

Fig. 5- 10 Redesigned harmonic lens simulation results of the side view of harmonic lens

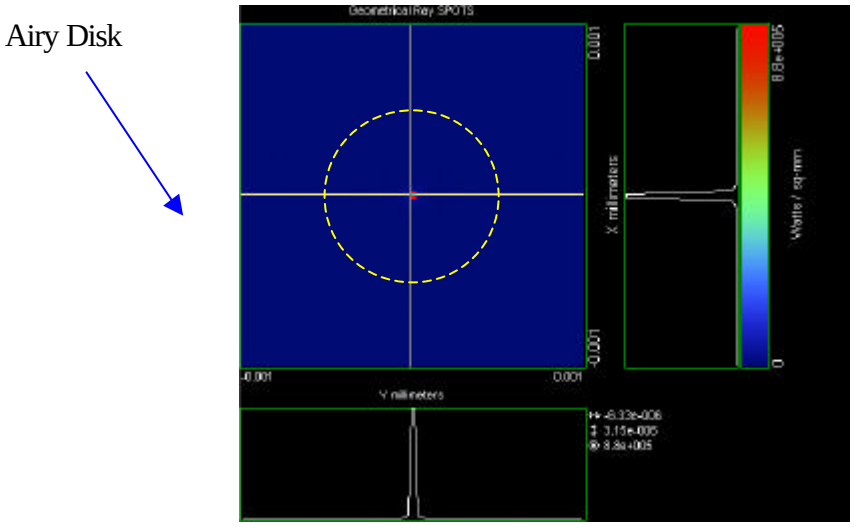

Fig. 5- 11 The density distribution of the redesigned harmonic lens simulated by using geometrical ray-tracing

The volume of this kind of objective lens is calculated by summing the individual segment volume. With the aspheric shape equation (Eq. 2-12), the volume of the objective lens is calculated to be 1.91×10^{-6} cm^3.

This approach is feasible to generate a thinner harmonic lens, and the volume of the system can be reduced. However, when the thickness becomes smaller, the

diffraction is more serious. As a result, the light intensity in the center of the spot is reduced due to the redistribution of energy, and the effective spot size will be increased. The diffraction performance of the overall harmonic lens is shown in Fig. 5-12, where the dash circle indicates the diffraction limits and the full width at half maximum is about 1 μm which meets the specification of DVD.

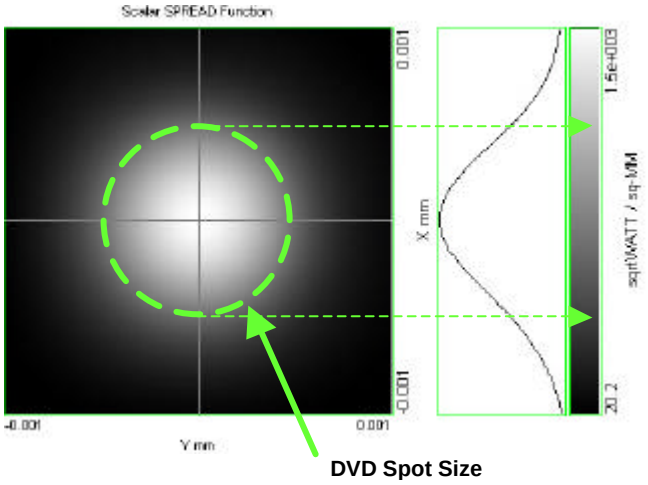

Fig. 5- 12 The diffraction performance of the harmonic lens

5.4.3 Tolerance analyses of harmonic lens for gray-scale lithography

When we use the gray-scale mask to fabricate a harmonic lens, two important issues which should be considered are (1) the time of exposure and (2) the number of shots. The insufficient time of exposure causes the shallow etching depth and the rough surface. When we change the number of shot of gray-scale lithography to modulate the slope of the lens profile, the slope is restricted to some values. Thus, the vertical surface of each segment shown in Fig. 5- 13 is not easily to be fabricated. These non-sharp surfaces caused by gray-scale lithography will induce the stray light and reduce the illumination at the focal point. Therefore, the fabrication tolerance should be analyzed. In the following subsections, we will discuss the tolerance of gray-scale lithography by calculating the radius of spot size.

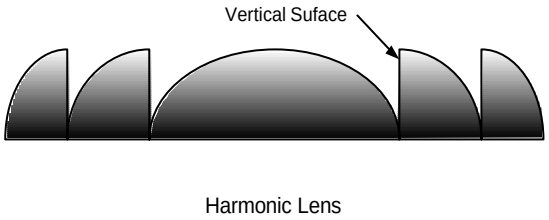

Fig. 5- 13 Schematic diagram of harmonic lens

(a) Shallow etching depth and rough surface

The shallow etching depth and rough surface are due to insufficient exposure of lithography. The deviations of designed and fabricated lens profiles are related to the lens parameters, including the thickness, the curvature, and the conic constant. To determine the acceptable range of lens parameters, the root mean square (RMS) radius of focused spot smaller the Airy disk is taken as the criterion. Since the harmonic lens is composed of redesigned segments, the tolerances related to the aspheric lens parameters are affected by each segment. Consequently, the RMS spot radii of segment 1, 2, and 3 calculated by varying lens parameters are shown in Fig. 5- 14, Fig. 5- 15, and Fig. 5- 16, respectively. In these calculations, the edge thickness must be positive in practice while lens parameters are changed. The deference in thickness between the designed and fabricated harmonic lens is of less than 1 μm. The dashed area in these figures denotes the acceptable range of lens parameters.

Based on the simulation, the conclusions are given. The fourth zone has no geometrical aberrations (Fig. 5- 17) because the spot size is too small to be identified, as indicated in Fig. 5- 11. Among the four segments of harmonic lens, the dominate segment is the second because the spot size is close to the Airy disk while the spot sizes of other segments are much smaller than the Airy disk. Besides, the deviation of lens parameters causes the thickness alteration of 1 μm on the edge of each redesigned zone. Therefore, the fabrication error of the harmonic lens must be controlled within 1 μm to minimize the spot size.

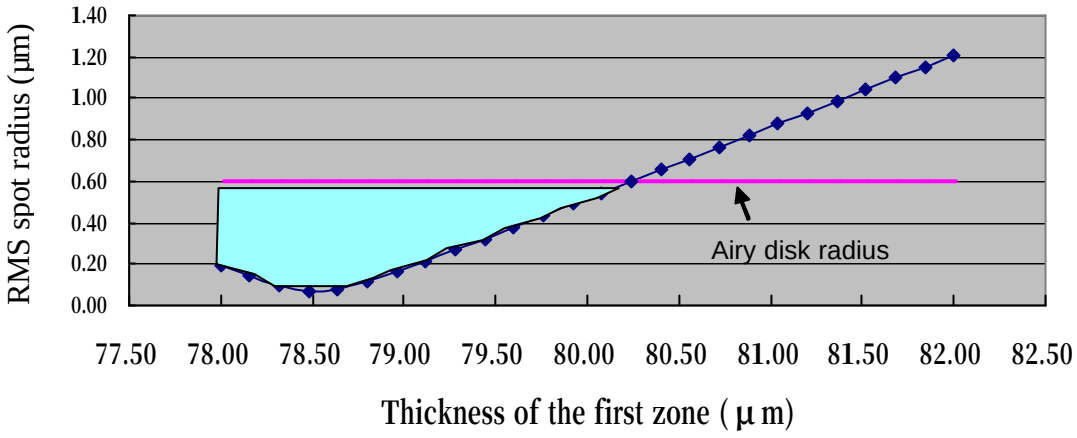

(a)

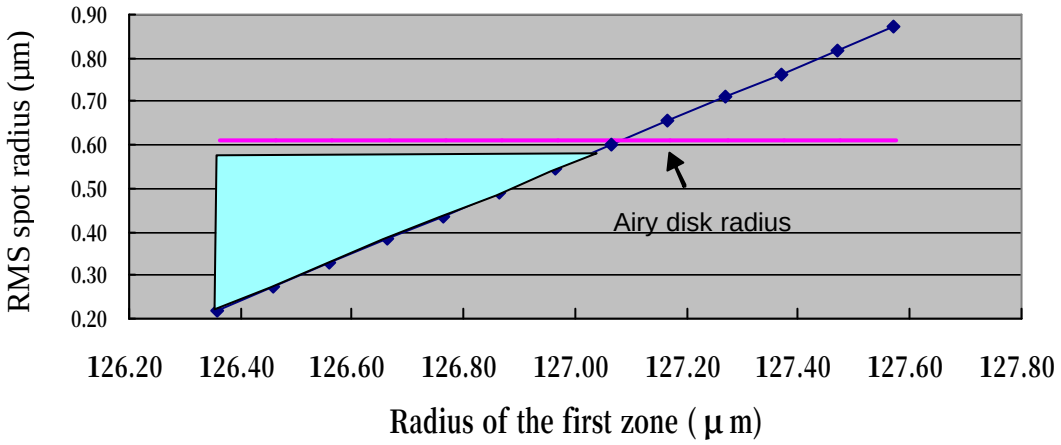

(b)

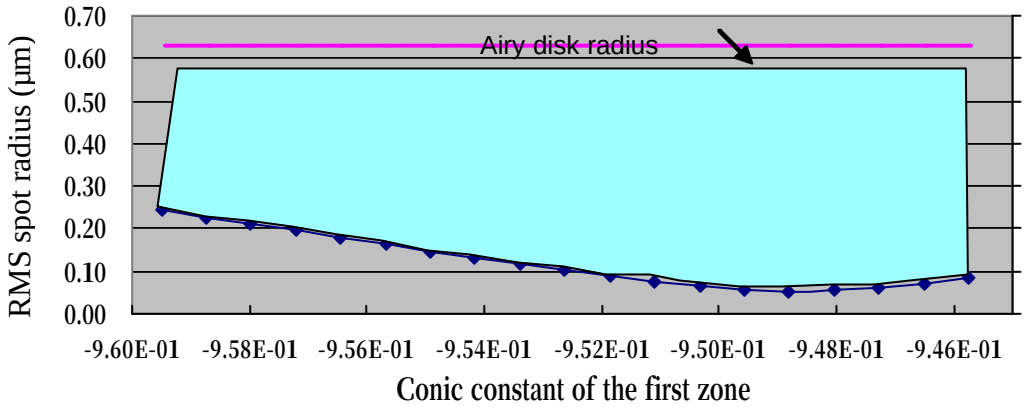

(c)

Fig. 5- 14 Root mean square (RMS) radius of focused spot as a function of (a) thickness, (b) radius, and (c) conic constant of the first segment of the harmonic lens

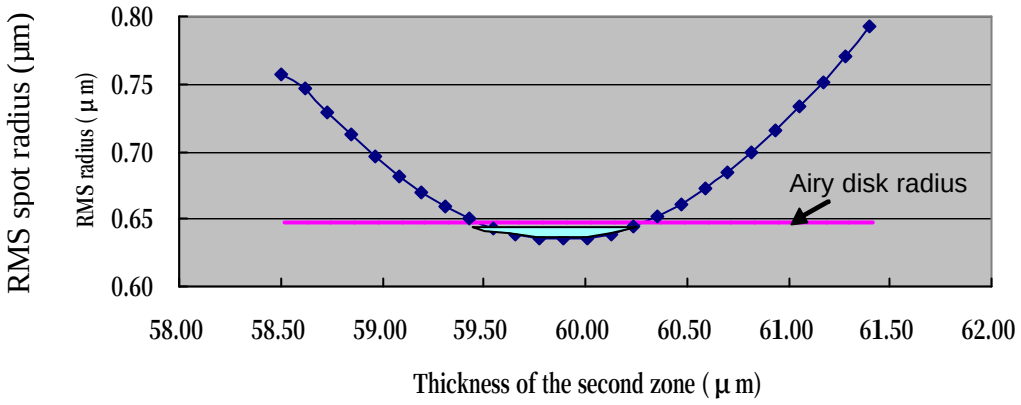

(a)

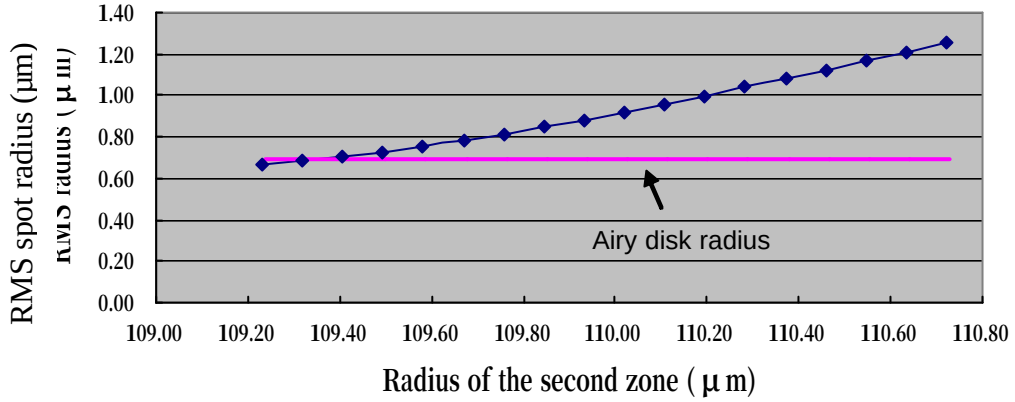

(b)

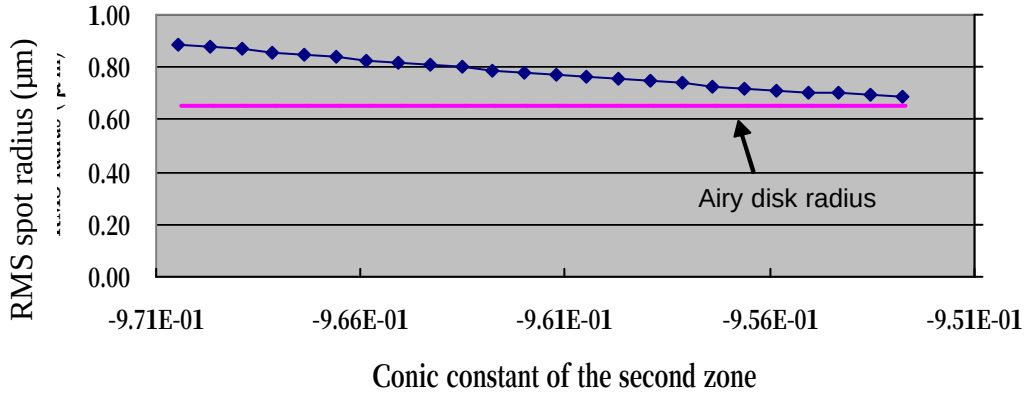

(c)

Fig. 5- 15 Root mean square (RMS) radius of focused spot as a function of (a) thickness, (b) radius, and (c) conic constant of the second segment of the harmonic lens

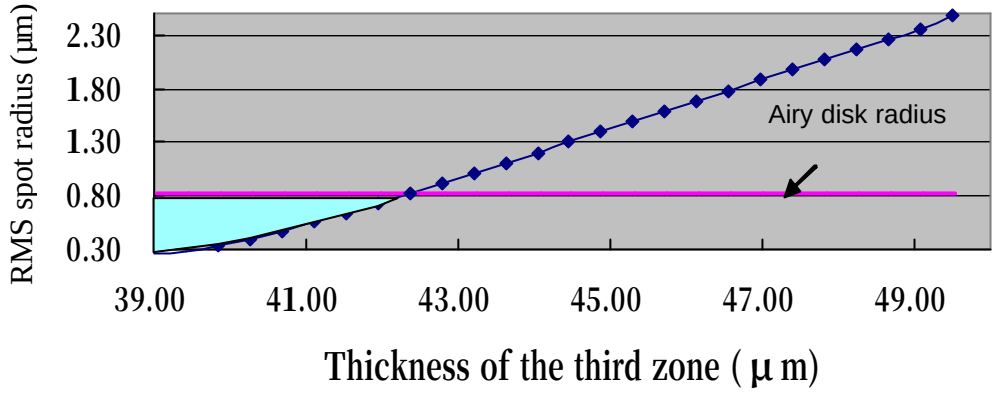

(a)

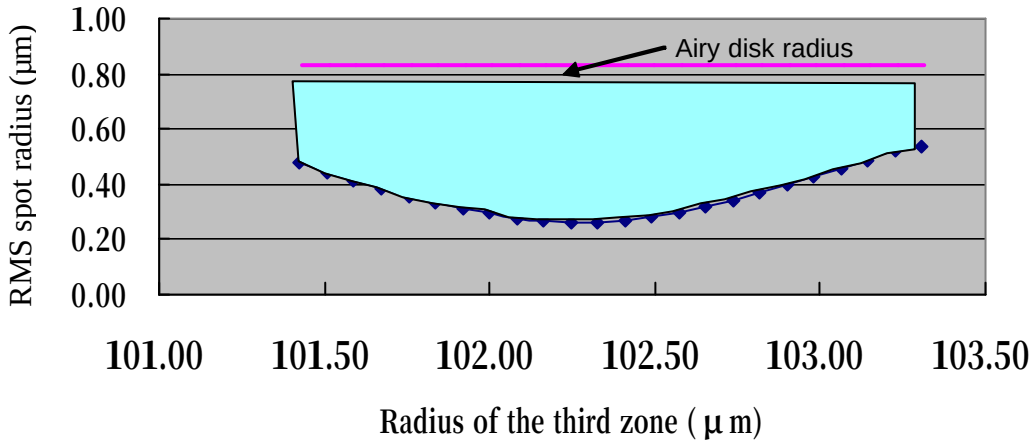

(b)

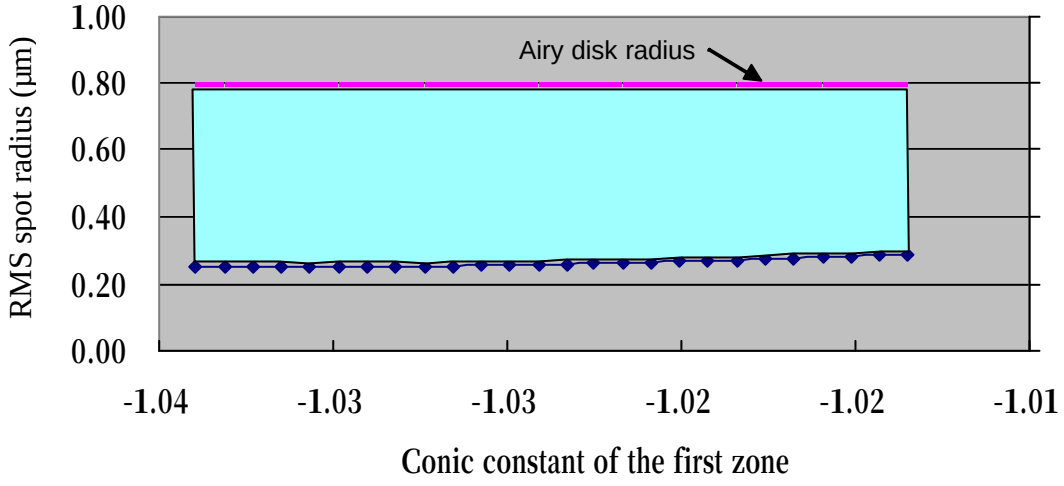

(c)

Fig. 5- 16 Root mean square (RMS) radius of focused spot as a function of (a) thickness, (b) radius, and (c) conic constant of the third segment of the harmonic lens

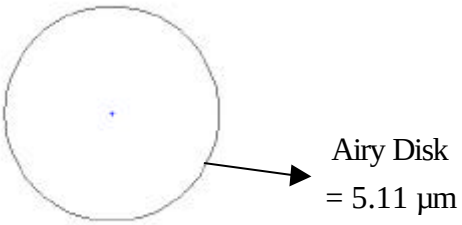

Fig. 5- 17 Spot size of the fourth zone

(b) The maximum slope of the steep profile

The second tolerance is related to the oblique surface due to the gray-scale lithography. The reason for the aberration and illumination reduction of the surface with an angle ? to the normal direction of the lens is shown in Fig. 5- 18. The ray indicated in dash line is bent outward by the oblique surface of harmonic lens when passing though the interface of air and lens.

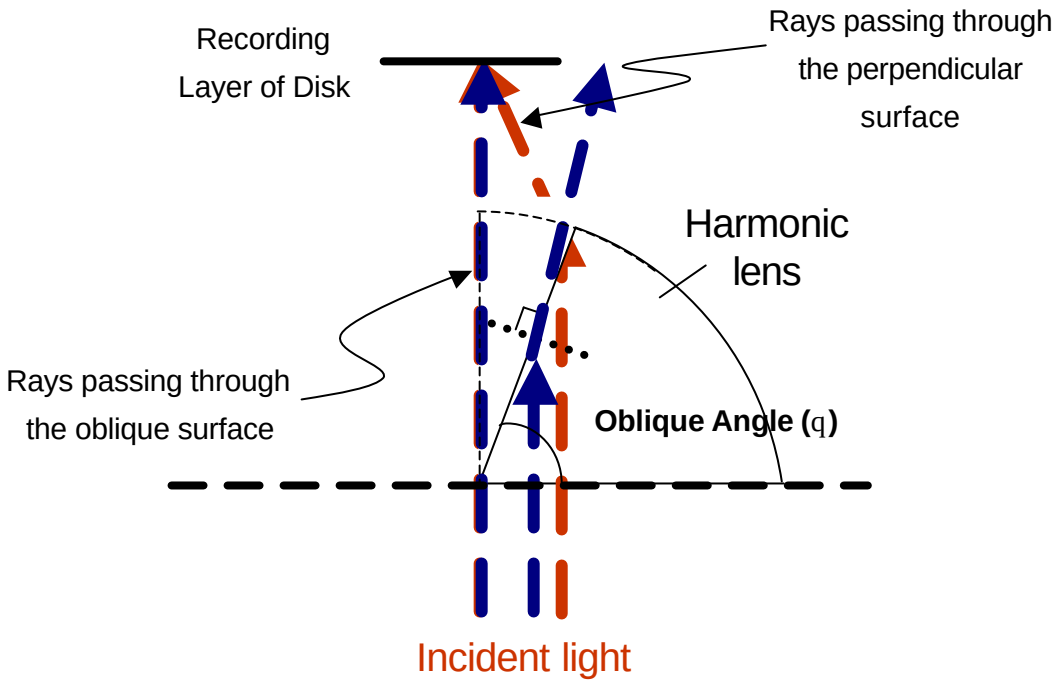

Fig. 5- 18 Schematic diagram of aberrations due to the oblique surface

The illumination of harmonic lens is a function of the angle ?. Relations between the normalized intensity and the tilt angle of the inner facet of each zone are shown in Fig. 5- 19. In Fig. 5- 19, as the tilt angle increases, the flux of the focused light in the recording layer decreases. For the maximum oblique angle ? = 65° of gray-scale mask, the normalized flux will be reduced to 95 %.

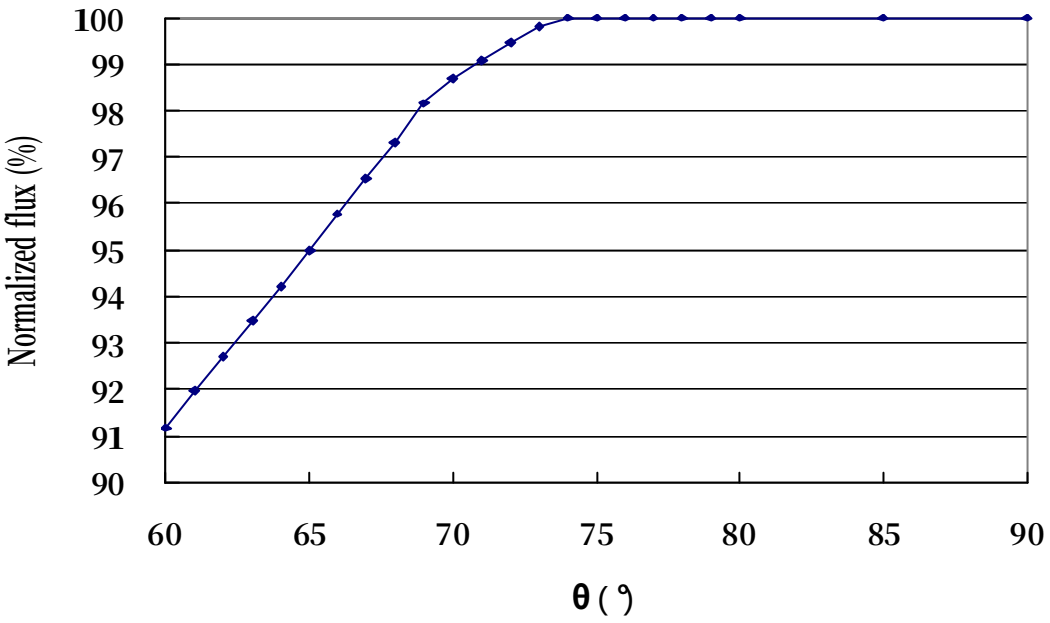

Fig. 5- 19 The relationship between the normalized flux in the recording layer and the tilt angles of the inner edge of each zone

5.5 Conclusion

The shape of an aspheric surface can be fabricated with gray-scale mask. A near diffraction-limited objective lens of minimal possible size of 1.91×10^{-6} cm^3, with the consideration of the given DVD pickup specification, has been designed. However, the lens thickness is too large to fabricate. To further reduce the lens thickness, one way is to use Fresnel lens. The lens profile, including zone diameter and continuous relief of each zone segment was derived. However, the linewidth of the Fresnel lens

was found to be too narrow for fabrication.

To solve the issues of too large thickness and too fine linewidth, the harmonic diffractive lens has been exploited. The traditional method of slicing refractive lens into harmonic diffractive lens introduces aberration. A new design approach of redesigning the shape of each zone has been proposed to address this issue. The simulation results confirm the feasibility of this approach. The resulted objective has a diameter of 260 μm and a working distance of 50 μm, a NA of 0.634 with a beam width of 210 μm. The focused spot size on the disk surface is 0.531 μm. From the geometrical shape of the objective lens, the volume of lens was estimated to be 1.91×10^{-6} cm^3. The distance between the fan-out grating and the objective lens is about 2 mm.